Postprint version of paper published in Chemical Engineering Science 2013, vol. 104, p. 285–293.
The content is identical to the published paper, but without the final typesetting by the publisher.

Analysis of smearing-out in contribution plot based fault isolation for Statistical Process Control

Pieter Van den Kerkhof[a], Jef Vanlaer[a], Geert Gins[a], Jan F.M. Van Impe[a,*]

[a] *Chemical and Biochemical Process Technology and Control (BioTeC), Department of Chemical Engineering, KU Leuven, W. de Croylaan 46, B-3001 Heverlee (Leuven), Belgium*

Abstract

This paper studies the smearing effect encountered in contribution plot based fault isolation, i.e., the influence of faulty variables on the contributions of non-faulty variables. Since the generation of contribution plots requires no a priori information about the detected disturbance (e.g., historical faulty data), it is a popular fault isolation technique in Statistical Process Control (SPC). However, Westerhuis *et al.* demonstrated that contributions suffer from fault smearing [1]. As a consequence, variables unaffected by the fault may be highlighted and faulty variables obscured during the contribution analysis. This paper presents a thorough analysis of the smearing effect for three general contribution computation methods: Complete Decomposition, Partial Decomposition and Reconstruction-Based contributions. The analysis shows that (*i*) smearing is present in all three methods, (*ii*) smearing depends on the chosen number of principal components of the underlying PCA or PLS model and (*iii*) the extent of smearing increases for variables correlated in the training data for a well-chosen model order. The effect of smearing on the isolation performance of single and multiple sensor faults of various magnitudes is studied and illustrated using a simulation case study. The results indicate that correct isolation with contribution plots is not guaranteed for multiple sensor faults. Furthermore, contribution plots only outperform univariate fault isolation for single sensor faults with small magni-

*Corresponding author

Email addresses: pieter.vandenkerkhof@cit.kuleuven.be (Pieter Van den Kerkhof), jef.vanlaer@cit.kuleuven.be (Jef Vanlaer), geert.gins@cit.kuleuven.be (Geert Gins), jan.vanimpe@cit.kuleuven.be (Jan F.M. Van Impe)

Postprint of manuscript accepted for Chemical Engineering Science

Journal homepage: http://www.journals.elsevier.com/chemical-engineering-science
Original file available at: http://dx.doi.org/10.1016/j.ces.2013.08.007

Postprint version of paper published in Chemical Engineering Science 2013, vol. 104, p. 285–293.
The content is identical to the published paper, but without the final typesetting by the publisher.

tudes. For multiple sensor faults, univariate fault isolation exhibits a significantly larger correct fault isolation rate. Based on the smearing analysis and the specific results for sensor faults, the authors advise to use contributions only if a sound physical interpretation of the principal components is available. Otherwise multivariate detection followed by univariate fault isolation is recommended.

Keywords: Process control, Mathematical modelling, Chemical processes, Fault detection/isolation, Contribution plots, Remediation

---

1. Introduction

Abnormal event management is of central importance to the process industries. Early detection and diagnosis of process faults permit timely interventions to keep the process within a safe controllable operating region and avoids production loss associated with the abnormal situation. Statistical Process Control (SPC) is a set of data-based techniques for process monitoring, fault detection and fault diagnosis. Due to the abundance of sensors in today's process plants, extensive historical databases containing frequent measurements of online sensors on hundreds of variables are becoming a commodity for process engineers. Therefore, employing SPC to exploit these existing databases has tremendous potential and has already resulted in a number of applications in industries as diverse as the petrochemical [2, 3], (bio)chemical [4, 5, 6], pulp and paper [7] and steel [8, 9] industries.

The basic concept of SPC is the statistical comparison of the current process measurements with historical data obtained under Normal Operating Conditions (NOC). Process behavior not included in the NOC data is detected by fault detection statistics. The process is monitored using control charts which depict the value of the statistic and corresponding control limits for normal operation at each time point.

Statistical projection methods such as Principal Component Analysis (PCA [10]) and Partial Least Squares (PLS [11]) greatly simplify fault detection by reducing the multivariate and typically heavily correlated sensor data to a smaller set of uncorrelated latent variables. The successful application of PCA and PLS has been reported extensively in the literature and has become a standard approach to SPC since its introduction in the early nineties [12, 13]. Progress has been made in improving fault detection performance by including process dynamics (e.g., dynamic PCA/PLS [14, 15],

Journal homepage: http://www.journals.elsevier.com/chemical-engineering-science
Original file available at: http://dx.doi.org/10.1016/j.ces.2013.08.007

Postprint version of paper published in Chemical Engineering Science 2013, vol. 104, p. 285–293.
The content is identical to the published paper, but without the final typesetting by the publisher.

auto-regressive PCA [16]) or by non-linear extensions (e.g., kernel PCA [17], kernel PLS [18]).

Upon detection of a process disturbance, the multivariate control charts do not provide any information about the root cause of the abnormal situation. If a sufficient amount of historical data of all of the process faults is available, classification methods can achieve conclusive diagnosis results by assigning the fault class to which the new measured data most resembles. However, as the process is designed and controlled to remain in the normal operating region, the availability of such data is often a bottleneck for developing an adequate classifier.

Alternatively, the underlying PCA or PLS model can be investigated by examining contribution plots, which chart the contribution of each variable to the out-of-control statistic [19]. The generation of contribution plots requires no historical data of the detected process disturbance, but process knowledge is necessary for interpreting the contribution pattern. Because of its ease of implementation and the absence of a need for historical faulty data, contribution plots are by far the most popular approach to find the cause of an alarm signal in SPC and have found extensive use in applications (see e.g., [4, 20, 3, 6]). Despite their popularity, there is still room for improvement. Westerhuis *et al.* used a simple example to illustrate that faulty variables can increase the contribution of variables not influenced by the fault [1]. This 'smearing' effect quickly leads to ambiguous diagnosis results for complex process faults. Moreover, different contribution computation methods were proposed in the literature each having different smearing properties. Hence, a profound understanding of the smearing effect is imperative for the choice of a contribution computation technique and a correct interpretation of the fault isolation results.

The goal of this paper is to provide a deeper insight into the smearing effect for contribution plots. The remainder of this paper is structured as follows. Section 2 contains a concise description of contribution computation. Section 3 presents an analysis of the causes of contribution smearing for three popular general types of contribution computation methods. In Section 4 the influence of smearing on fault isolation is further studied for the case of sensor faults and referenced against isolation based directly on the pretreated data. Section 5 ties the analysis and case study results together to present a different view on contribution smearing and, finally, Section 6 draws some conclusions.

Journal homepage: http://www.journals.elsevier.com/chemical-engineering-science
Original file available at: http://dx.doi.org/10.1016/j.ces.2013.08.007

Postprint version of paper published in Chemical Engineering Science 2013, vol. 104, p. 285–293.
The content is identical to the published paper, but without the final typesetting by the publisher.

2. Contribution plots

Control charts alarm when an abnormal situation has been encountered, but do not provide any further information about the cause. Therefore, variable contributions to the out-of-control fault detection statistic are plotted to extract useful information for fault diagnosis [19]. Contribution plots rely on the investigation of the underlying statistical projection method. This paper focuses on basic PCA for ease of explanation and because of its popularity in industrial applications. The derived formulas can be readily extended to other statistical projection methods (see, e.g., Westerhuis *et al.* [1]). Section 2.1 briefly describes the basics of PCA based process monitoring and Section 2.2 discusses the theory of contribution computation.

2.1. PCA based monitoring

Consider an industrial data set consisting of m measurements on n variables organized in an $m \times n$ data matrix $\mathbf{X}$. Before applying PCA, each column of $\mathbf{X}$ is scaled to zero mean and unit variance (i.e., auto-scaling). For the remainder of this paper, the data is assumed to be auto-scaled. PCA divides the original $\mathcal{R}^n$ measurement space into a model space spanned by principal components (the model hyperplane) and a residual space [10, 21]. The principal components are obtained from the eigen-decomposition of the covariance matrix $\mathbf{S}$ of $\mathbf{X}$

$$\mathbf{S} = \frac{1}{m-1}\mathbf{X}^{\mathrm{T}}\mathbf{X} \tag{1}$$

$$= \begin{bmatrix}\mathbf{P} & \tilde{\mathbf{P}}\end{bmatrix} \begin{bmatrix}\mathbf{\Lambda} & \mathbf{0} \\ \mathbf{0} & \tilde{\mathbf{\Lambda}}\end{bmatrix} \begin{bmatrix}\mathbf{P} & \tilde{\mathbf{P}}\end{bmatrix}^{\mathrm{T}} \tag{2}$$

where $\mathbf{P} \in \mathcal{R}^{n\times r}$ contains the r eigenvectors of $\mathbf{S}$ associated with the r largest eigenvalues contained in a diagonal matrix $\mathbf{\Lambda} \in \mathcal{R}^{r\times r}$ and $\tilde{\mathbf{P}} \in \mathcal{R}^{n\times n-r}$ holds the eigenvectors corresponding to the remaining eigenvalues contained in a diagonal matrix $\tilde{\mathbf{\Lambda}} \in \mathcal{R}^{n-r\times n-r}$. The number of retained principal components r is decided by the user. The columns of $\mathbf{P}$ and $\tilde{\mathbf{P}}$ span the model hyperplane and residual space respectively. A measurement vector $\mathbf{x} \in \mathcal{R}^n$ can therefore be decomposed into two vectors

$$\hat{\mathbf{x}} = \mathbf{P}\mathbf{P}^{\mathrm{T}}\mathbf{x} \tag{3}$$

$$\tilde{\mathbf{x}} = \tilde{\mathbf{P}}\tilde{\mathbf{P}}^{\mathrm{T}}\mathbf{x} \tag{4}$$

Journal homepage: http://www.journals.elsevier.com/chemical-engineering-science
Original file available at: http://dx.doi.org/10.1016/j.ces.2013.08.007

Postprint version of paper published in Chemical Engineering Science 2013, vol. 104, p. 285–293.
The content is identical to the published paper, but without the final typesetting by the publisher.

with $\hat{\mathbf{x}}$ and $\tilde{\mathbf{x}}$ the projections of $\mathbf{x}$ on the model and residual spaces, respectively. A measurement vector $\mathbf{x}$ can be represented in a new coordinate system defined by the columns of $\mathbf{P}$

$$\mathbf{t} = \mathbf{x}^{\mathrm{T}}\mathbf{P} \tag{5}$$

where $\mathbf{t} \in \mathcal{R}^{r\times 1}$ contains the so-called scores of $\mathbf{x}$ that represent $\mathbf{x}$ by a reduced set of r uncorrelated variables.

The measurement vector $\mathbf{x}$ is subjected to fault detection by computing fault detection indices. The general formula for quadratic fault detection indices is

$$\mathrm{Index}\,(\mathbf{x}) = \|\mathbf{x}\|^2_{\mathbf{M}} = \mathbf{x}^{\mathrm{T}}\mathbf{M}\mathbf{x} \tag{6}$$

where $\mathbf{M}$ depends on the specific fault detection statistic. For the popular Squared Prediction Error (SPE) and Hotelling's T^2 statistics, $\mathbf{M}$ is equal to

$$\mathbf{M}_{\mathrm{SPE}} = \tilde{\mathbf{P}}\tilde{\mathbf{P}}^{\mathrm{T}}, \tag{7}$$

$$\mathbf{M}_{\mathrm{T}^2} = \mathbf{P}\mathbf{\Lambda}^{-1}\mathbf{P}^{\mathrm{T}}. \tag{8}$$

The matrices $\mathbf{M}_{\mathrm{SPE}}$ and $\mathbf{M}_{\mathrm{T}^2}$ are symmetric and positive (semi-)definite. $\mathbf{M}_{\mathrm{SPE}}$ is also idempotent. The corresponding Upper Control Limits (UCL) with tolerance level α are given by

$$\mathrm{UCL}_{\mathrm{SPE}} = \frac{\sigma^2_{\mathrm{SPE}}}{2\mu_{\mathrm{SPE}}}\chi^2(2\mu^2_{\mathrm{SPE}}/\sigma^2_{\mathrm{SPE}};\alpha) \tag{9}$$

$$\mathrm{UCL}_{\mathrm{T}^2} = \chi^2(r;\alpha) \tag{10}$$

where the mean and variance of the SPE statistic over all training samples are denoted by μ_{SPE} and σ^2_{SPE} and $\chi^2_{\mathrm{SPE}}(2\mu^2_{\mathrm{SPE}}/\sigma^2_{\mathrm{SPE}};\alpha)$ and $\chi^2(r;\alpha)$ are the upper critical values of a χ^2-distribution with respectively $2\mu^2_{\mathrm{SPE}}/\sigma^2_{\mathrm{SPE}}$ and r degrees of freedom at a specified tolerance level α.

2.2. Contribution computation

The use of contribution plots for Statistical Process Control (SPC) was introduced by MacGregor *et al.* for batch processes in order to investigate the underlying PCA or PLS model when a fault detection statistic exceeds its control limit [22, 23]. MacGregor *et al.* decompose the fault detection statistic into a sum of terms, each associated with one variable, called contributions. The assumption behind contribution computation is that variables

Journal homepage: http://www.journals.elsevier.com/chemical-engineering-science
Original file available at: http://dx.doi.org/10.1016/j.ces.2013.08.007

Postprint version of paper published in Chemical Engineering Science 2013, vol. 104, p. 285–293.
The content is identical to the published paper, but without the final typesetting by the publisher.

associated with the fault exhibit large contributions. In this case, a contribution plot enables engineers and operators to focus their attention on a small subset of variables and therefore facilitates the diagnostic task.

Upon detection, the contribution of each variable to the fault detection statistic is generated to obtain diagnostic information. As there is no unique way to decompose a fault detection statistic into a sum of terms each assigned to a single variable, various authors proposed different formulas for contribution computation. Alcala and Qin unified these into three general methods: complete decomposition, partial decomposition and reconstruction-based contributions [24].

2.2.1. Complete decomposition (CD)

The CD contribution of the i-th variable is defined by Alcala and Qin as

$$\mathrm{CD}_i = \left(\xi_i^{\mathrm{T}} \mathbf{M}^{\frac{1}{2}} \mathbf{x}\right)^2 \tag{11}$$

where ξ_i is the i-th column of the $n \times n$ identity matrix [24]. CD contributions are always positive and their sum is equal to the value of the corresponding statistic.

2.2.2. Partial decomposition (PD)

Alcala and Qin [24] define the PD contribution of the i-th variable as

$$\mathrm{PD}_i = \mathbf{x}^{\mathrm{T}} \mathbf{M} \xi_i \xi_i^{\mathrm{T}} \mathbf{x}. \tag{12}$$

As for CD contributions, the sum of the PD contributions equals the value of the corresponding fault detection statistic. However, contrary to CD contributions, PD contributions can attain negative values. When a variable is equal to its mean or expected value, i.e., $\xi_i^{\mathrm{T}} \mathbf{x} = x_i = 0$, its PD contribution is equal to zero.

2.2.3. Reconstruction-Based (RB)

RB contributions were proposed in [25]. In this approach, each variable x_i is reconstructed (x_i^{rec}) based on the remaining $n-1$ variables and the PCA model. The amount of reconstruction $f_i = x_i^{rec} - x_i$ is then used to obtain the RB contributions

$$\mathrm{RB}_i = \mathrm{Index}\left(\xi_i f_i\right) \tag{13}$$

$$= \left\| \xi_i f_i \right\|_{\mathbf{M}}^2 . \tag{14}$$

Journal homepage: http://www.journals.elsevier.com/chemical-engineering-science
Original file available at: http://dx.doi.org/10.1016/j.ces.2013.08.007

Postprint version of paper published in Chemical Engineering Science 2013, vol. 104, p. 285–293.
The content is identical to the published paper, but without the final typesetting by the publisher.

RB contributions are always positive. Unlike CD and PD contributions, their sum is not guaranteed to be equal to the value of the corresponding statistic.

Alcala and Qin based their RB method on the work of Dunia and Qin [26] and Yue and Qin [27]. In these works, the reconstructed variable is found by minimizing the fault index of the reconstructed measurement vector

$$\text{Index}\left(\mathbf{x} - \xi_i f_i\right) = \left\|\mathbf{x} - \xi_i f_i\right\|_{\mathbf{M}}^2 . \tag{15}$$

Minimizing Eq. 15 with respect to f_i yields

$$f_i = \left(\xi_i^{\mathrm{T}} \mathbf{M} \xi_i\right)^{-1} \xi_i^{\mathrm{T}} \mathbf{M} \mathbf{x}. \tag{16}$$

Substituting this expression for f_i into the general definition of RB contributions results in

$$\mathrm{RB}_i = \frac{\left(\xi_i^{\mathrm{T}} \mathbf{M} \mathbf{x}\right)^2}{\xi_i^{\mathrm{T}} \mathbf{M} \xi_i} \tag{17}$$

which is the definition of the third general method for contribution calculation according to Alcala and Qin [24]. However, the above definition is not general and is only valid when reconstructing a variable based on minimizing the corresponding fault index, which is a form of projection-based reconstruction. Reconstructing a variable is equal to treating the variable as missing data and estimating its value based on the remaining variables. Arteaga and Ferrer provide an overview for estimating missing variables in [28] and minimization of the SPE index is one of the various reconstruction methods provided. Hence, it is possible to obtain different formulations for RB contributions depending on the reconstruction method used to compute the amount of reconstruction f_i in Eq. 14. For example, Lieftucht *et al.* proposed regression-based reconstruction to overcome some problems associated with projection-based reconstruction [29, 30]. For the remainder of this paper, Eq. 17 will be used for computation of RB contributions, reflecting the original approach of Alcala and Qin [25, 24].

3. The smearing effect

Westerhuis *et al.* were the first to illustrate that faulty variables increase the contribution of variables not influenced by the fault [1]. As a consequence, the effect of a fault is smeared out over the different contributions and the difference between contributing and non-contributing variables decreases. Therefore, Yoon and MacGregor argue that contribution plots are

Journal homepage: http://www.journals.elsevier.com/chemical-engineering-science
Original file available at: http://dx.doi.org/10.1016/j.ces.2013.08.007

Postprint version of paper published in Chemical Engineering Science 2013, vol. 104, p. 285–293.
The content is identical to the published paper, but without the final typesetting by the publisher.

only appropriate for simple process faults, i.e., faults with a specific fault source and of which the effect is not propagated to other variables [31]. This section analyzes the smearing behavior of CD, PD and RB contributions to provide a deeper understanding of the cause and nature of contribution smearing.

3.1. Smearing of CD contributions

Substituting $\mathbf{M}$ in Eq. 11 by $\tilde{\mathbf{P}}\tilde{\mathbf{P}}^{\mathrm{T}}$ for the SPE statistic and $\mathbf{P}\mathbf{\Lambda}^{-1}\mathbf{P}^{\mathrm{T}}$ for the T^2 statistic yields their CD contributions

$$\mathrm{CD}_i^{\mathrm{SPE}} = \left(\xi_i^{\mathrm{T}}\left(\tilde{\mathbf{P}}\tilde{\mathbf{P}}^{\mathrm{T}}\right)^{\frac{1}{2}}\mathbf{x}\right)^2 \tag{18}$$

$$\mathrm{CD}_i^{\mathrm{T}^2} = \left(\xi_i^{\mathrm{T}}\left(\mathbf{P}\mathbf{\Lambda}^{-1}\mathbf{P}^{\mathrm{T}}\right)^{\frac{1}{2}}\mathbf{x}\right)^2. \tag{19}$$

By using the idempotent property of $\tilde{\mathbf{P}}\tilde{\mathbf{P}}^{\mathrm{T}}$ and Eq. 4, the CD contributions to the SPE statistic reduce to

$$\mathrm{CD}_i^{\mathrm{SPE}} = \left(\xi_i^{\mathrm{T}}\tilde{\mathbf{P}}\tilde{\mathbf{P}}^{\mathrm{T}}\mathbf{x}\right)^2 \tag{20}$$

$$= \left(\xi_i^{\mathrm{T}}\tilde{\mathbf{x}}\right)^2 \tag{21}$$

$$= \tilde{x}_i^2. \tag{22}$$

The above derivation demonstrates that the CD contributions to the SPE statistic are equal to the squared components of the residual vector $\tilde{\mathbf{x}}$ along each axis of the original measurement space. The residual vector is computed by projecting the measurement vector on the residual subspace and expressing the resulting vector in the original coordinates. The compression to a smaller number of subspace variables and subsequent expansion back to the measurement space enables faulty and non-faulty variables to interact which is the fundamental cause of contribution smearing.

For the T^2 statistic, Eq. 19 can be rewritten as

$$\mathrm{CD}_i^{\mathrm{T}^2} = \left(\xi_i^{\mathrm{T}}\mathbf{P}\mathbf{\Lambda}^{-\frac{1}{2}}\mathbf{P}^{\mathrm{T}}\mathbf{x}\right)^2 \tag{23}$$

$$= \left(\xi_i^{\mathrm{T}}\mathbf{P}\mathbf{\Lambda}^{-\frac{1}{2}}\mathbf{t}^{\mathrm{T}}\right)^2. \tag{24}$$

To obtain the CD contributions to the T^2 statistic, $\mathbf{x}$ is projected onto the model plane to obtain the scores $\mathbf{t}$. Each score is scaled by its standard deviation before expressing the score vector in the original measurement space.

Journal homepage: http://www.journals.elsevier.com/chemical-engineering-science
Original file available at: http://dx.doi.org/10.1016/j.ces.2013.08.007

Postprint version of paper published in Chemical Engineering Science 2013, vol. 104, p. 285–293.
The content is identical to the published paper, but without the final typesetting by the publisher.

Similar to the CD contributions to the SPE index, the compression and subsequent expansion enables faulty and non-faulty variables to interact and causes the smearing effect.

To gain further insight into the smearing phenomenon, it is instructive to rewrite the two contribution formulas (Eqs. 18, 19) in a different form. At the mathematical core of each contribution formula is a simple linear combination of the measured variables. The CD contributions to the SPE and T^2 statistic can be rewritten as

$$\mathrm{CD}_i^{\mathrm{SPE}} = \left(\alpha_i x_i + \sum_{j=1, j\neq i}^{n} \gamma_{ij} x_j \right)^2 \tag{25}$$

$$\mathrm{CD}_i^{\mathrm{T}^2} = \left(\beta_i x_i + \sum_{j=1, j\neq i}^{n} \delta_{ij} x_j \right)^2 \tag{26}$$

where

$$\alpha_i = 1 - \sum_{l=1}^{r} p_{il}^2 \tag{27}$$

$$\beta_i = \sum_{l=1}^{r} \lambda_l^{-\frac{1}{2}} p_{il}^2 \tag{28}$$

$$\gamma_{ij} = -\sum_{l=1}^{r} p_{il} p_{jl} \tag{29}$$

$$\delta_{ij} = \sum_{l=1}^{r} \lambda_l^{-\frac{1}{2}} p_{il} p_{jl} \tag{30}$$

and p_{il} refers to the element at row i and column l of $\mathbf{P}$ i.e., the loading of x_i in the l-th principal component.

Three main conclusions can be drawn from the above equations. Firstly, faulty variables influence non-faulty ones through the linear combination of all variables (except the considered variable) at the core of these equations; the coefficients γ_{ij} and δ_{ij} quantify the amount of smearing. By using the PCA model of the NOC data, the coefficients of this linear combination can be computed. The actual amount of smearing then depends on the values

Journal homepage: http://www.journals.elsevier.com/chemical-engineering-science
Original file available at: http://dx.doi.org/10.1016/j.ces.2013.08.007

Postprint version of paper published in Chemical Engineering Science 2013, vol. 104, p. 285–293.
The content is identical to the published paper, but without the final typesetting by the publisher.

of the other variables and, hence, the specific fault. Secondly, as the coefficients γ_{ij} and δ_{ij} depend on the retained number of principal components r, the contribution pattern depends on the selected model order of the PCA or PLS model. Various methods for model order selection exist and their influence on contribution plot based fault isolation is rarely, if ever, considered. Finally, since correlated variables have similar loadings in the different principal components, the extent of smearing between variables tends to increase, provided the model order r is well-chosen to capture the underlying correlations without describing the noise. Hence, while a data plot at the moment of detection will only show increased values for variables directly influenced by the detected fault, contribution plots will also show increased values for those variables correlated with the latter variables. In the specific case of CD contributions, the influence of variable x_j on the contribution of x_i is equal to the influence of x_i on the contribution of x_j, i.e., symmetrical smearing. This is clear from the expressions of γ_{ij} and δ_{ij} since $\gamma_{ij} = \gamma_{ji}$ and $\delta_{ij} = \delta_{ji}$.

3.2. Smearing of PD contributions

The PD contributions can be obtained by substituting $\mathbf{M}$ in Eq. 12 with $\tilde{\mathbf{P}}\tilde{\mathbf{P}}^{\mathrm{T}}$ for the SPE statistic and $\mathbf{P}\boldsymbol{\Lambda}^{-1}\mathbf{P}^{\mathrm{T}}$ for the T^2 statistic, yielding

$$\mathrm{PD}_i^{\mathrm{SPE}} = \mathbf{x}^{\mathrm{T}}\tilde{\mathbf{P}}\tilde{\mathbf{P}}^{\mathrm{T}}\xi_i\xi_i^{\mathrm{T}}\mathbf{x} \tag{31}$$

$$\mathrm{PD}_i^{\mathrm{T}^2} = \mathbf{x}^{\mathrm{T}}\mathbf{P}\boldsymbol{\Lambda}^{-1}\mathbf{P}^{\mathrm{T}}\xi_i\xi_i^{\mathrm{T}}\mathbf{x}. \tag{32}$$

The expression for the SPE statistics contributions (Eq. 31) can be rearranged by substituting Eq. 4 to obtain

$$\mathrm{PD}_i^{\mathrm{SPE}} = \tilde{\mathbf{x}}^{\mathrm{T}}\xi_i\xi_i^{\mathrm{T}}\mathbf{x} \tag{33}$$

$$= \tilde{x}_i x_i. \tag{34}$$

A variable's PD contribution to the SPE statistic equals the product of its auto-scaled value x_i and corresponding residual $\tilde{x}_i$. Hence, the cause of contribution smearing is identical to CD contributions, though the smearing effect is mitigated by multiplication with the auto-scaled variable.

The latter equation (34) also provides insight into negative contributions. If the signs of x_i and $\tilde{x}_i$ differ, a negative contribution arises. Westerhuis *et al.* made the observation for a simple case study with only two variables that, if a negative PD contribution is obtained, setting the corresponding variable

Journal homepage: http://www.journals.elsevier.com/chemical-engineering-science
Original file available at: http://dx.doi.org/10.1016/j.ces.2013.08.007

Postprint version of paper published in Chemical Engineering Science 2013, vol. 104, p. 285–293.
The content is identical to the published paper, but without the final typesetting by the publisher.

x_i to zero increases the value of the fault detection statistic [1]. Using Eq. 34, the SPE statistic can be expressed as

$$\mathrm{SPE} = \sum_{i=1}^{n} \tilde{x}_i x_i \tag{35}$$

since the sum of the PD contributions equals the fault index. The above equation generalizes Westerhuis *et al.*'s observation to a data set containing n variables: setting a variable with a negative contribution to zero (i.e., its mean or expected value) in Eq. 35 increases the SPE statistic. Westerhuis *et al.* used their result to claim that negative contributions are not a special event and should not be considered for fault diagnosis, as only positive contributions force the fault detection statistic to be out-of-control [1]. However, according to Eq. 34, a variable with a negative contribution can have a large deviation from its mean value (x_i) and/or a large residual ($\tilde{x}_i$) despite the negative sign and therefore, in the authors' opinion, should not be discarded during fault isolation.

Reworking the expression for the T^2 statistic (Eq. 32) using Eq. 5

$$\mathrm{PD}_i^{\mathrm{T}^2} = \mathbf{t}\boldsymbol{\Lambda}^{-1}\mathbf{P}^{\mathrm{T}}\xi_i\xi_i^{\mathrm{T}}\mathbf{x} \tag{36}$$

$$= \left(\xi_i^{\mathrm{T}}\mathbf{P}\boldsymbol{\Lambda}^{-1}\mathbf{t}^{\mathrm{T}}\right) x_i, \tag{37}$$

results in the product of the mean centered variable x_i and a term similar to the square root of the T^2's CD contribution (Eq. 24). Although each score is scaled by its variance instead of its standard deviation, the same conclusions about smearing as in the CD case apply. The analysis of negative contributions to the T^2 statistic leads to similar results as the SPE statistic.

The formulas for the PD contributions can be rearranged as the product of the variable with a linear combination of all variables.

$$\mathrm{PD}_i^{\mathrm{SPE}} = x_i \left(\alpha_i x_i + \sum_{j=1, j\neq i}^{n} \gamma_{ij} x_j \right) \tag{38}$$

$$\mathrm{PD}_i^{\mathrm{T}^2} = x_i \left(\epsilon_i x_i + \sum_{j=1, j\neq i}^{n} \zeta_{ij} x_j \right) \tag{39}$$

Journal homepage: http://www.journals.elsevier.com/chemical-engineering-science
Original file available at: http://dx.doi.org/10.1016/j.ces.2013.08.007

Postprint version of paper published in Chemical Engineering Science 2013, vol. 104, p. 285–293.
The content is identical to the published paper, but without the final typesetting by the publisher.

where

$$\epsilon_i = \sum_{l=1}^{r} \lambda_l^{-1} p_{il}^2 \tag{40}$$

$$\zeta_{ij} = \sum_{l=1}^{r} \lambda_l^{-1} p_{il} p_{jl}. \tag{41}$$

The above equations lead to the same three conclusions as for the CD contributions: (*i*) the linear combination at the core of the equations evidences the presence of smearing, quantified by the coefficients γ_{ij} and ζ_{ij}, (*ii*) the contributions depend on the selected model order of the underlying PCA or PLS model and (*iii*) the extent of smearing between variables tends to increase as the variables are more correlated in the NOC data on the condition that the model order is high enough to adequately reflect the NOC covariance matrix. However, the premultiplication of x_i mitigates the smearing effect at the cost of the occurrence of counterintuitive negative contributions. Like CD contributions, PD contributions exhibit symmetrical smearing since $\gamma_{ij} = \gamma_{ji}$ and $\zeta_{ij} = \zeta_{ji}$.

3.3. Smearing of RB contributions

The concept of RB contributions is to reconstruct each variable based on the other variables. When reconstructing a non-faulty variable, some of the remaining variables are faulty and faulty information is used for reconstruction. Hence, smearing is present in RB contributions by definition.

Similar arithmetics as in the CD and PD cases lead to the following expressions for RB contributions

$$\mathrm{RB}_i^{\mathrm{SPE}} = \left(\alpha_i x_i + \sum_{j=1, j\neq i}^{n} \gamma_{ij} x_j \right)^2 / \alpha_i \tag{42}$$

$$\mathrm{RB}_i^{\mathrm{T}^2} = \left(\epsilon_i x_i + \sum_{j=1, j\neq i}^{n} \zeta_{ij} x_j \right)^2 / \epsilon_i. \tag{43}$$

The above expressions are very similar to the expressions for CD contributions (Eqs. 25 and 26) and the same conclusions about the presence of smearing, quantified by $\gamma_{ij}/\sqrt{\alpha_i}$ and $\zeta_{ij}/\sqrt{\epsilon_i}$, the effect of r and the influence of NOC correlations are drawn. Note that, unlike CD contributions, the influence of variable x_j on the contribution of x_i is not necessarily equal to the

Journal homepage: http://www.journals.elsevier.com/chemical-engineering-science
Original file available at: http://dx.doi.org/10.1016/j.ces.2013.08.007

Postprint version of paper published in Chemical Engineering Science 2013, vol. 104, p. 285–293.
The content is identical to the published paper, but without the final typesetting by the publisher.

influence of x_i on the contribution of x_j, i.e., asymmetrical smearing, since $\gamma_{ij}/\sqrt{\alpha_i} \neq \gamma_{ji}/\sqrt{\alpha_j}$ and $\zeta_{ij}/\sqrt{\epsilon_i} \neq \zeta_{ji}/\sqrt{\epsilon_j}$.

4. A case study: sensor faults

Sensor faults are, from a fault isolation point of view, the simplest faults that can happen in a process and therefore form a useful case study to investigate the effect of contribution smearing.

4.1. Theoretical results

Alcala and Qin studied sensor faults where the fault-free measurements are zero, i.e., equal to their mean or expected value (for a continuous process) or lying on the average trajectory (for batch processes), and the faulty sensor has a magnitude equal to f [25]. The faulty measurement vector is of the following form

$$\mathbf{x}_f = f\xi_j. \tag{44}$$

If the contribution of the faulty variable is greater than or equal to any other fault-free variables' contribution, the fault is isolated correctly. Alcala and Qin proved for this type of single sensor faults that correct isolation is guaranteed for the PD and RB contributions but not for CD contributions [25].

In this paper, the analysis is extended to multiple sensor faults, i.e., faults of the form

$$\mathbf{x}_{ff} = f\xi_j + \phi f\xi_k \tag{45}$$

where f is the magnitude of the sensor fault on variable j and $\phi \in \Re$ is a scalar to express the magnitude ϕf of the sensor fault on variable k ($j \neq k$). From the results of Alcala and Qin, correct isolation of multiple sensor faults with CD contributions is not guaranteed [25]. In the next two paragraphs, the isolatability of $\mathbf{x}_{ff}$ will be analyzed for the PD and RB contributions. Note that by the definition of $\mathbf{x}_f$ and $\mathbf{x}_{ff}$, isolation of these fault types based on the mean centered data instead of contributions is trivial since the only variables deviating from their expected value, i.e., zero, are the faulty variables.

Journal homepage: http://www.journals.elsevier.com/chemical-engineering-science
Original file available at: http://dx.doi.org/10.1016/j.ces.2013.08.007

Postprint version of paper published in Chemical Engineering Science 2013, vol. 104, p. 285–293.
The content is identical to the published paper, but without the final typesetting by the publisher.

Isolatability for PD contributions

To study the isolatability of multiple sensor faults, $\mathbf{x}_{ff}$ is substituted into the general expression for PD contributions (Eq. 12) yielding

$$\mathrm{PD}_i = \begin{cases} 0 & \text{if } i \neq j \wedge i \neq k \\ f^2\left(m_{jj} + \phi m_{kj}\right) & \text{if } i = j \\ f^2\left(\phi^2 m_{kk} + \phi m_{jk}\right) & \text{if } i = k \end{cases} . \tag{46}$$

where m_{ij} equals $\xi_i^{\mathrm{T}}\mathbf{M}\xi_j$, i.e., the element at the i-th row and j-th column of $\mathbf{M}$. Therefore, to guarantee isolatability, the contributions of the j-th and k-th variable must be greater than or equal to the contribution of any other variable

$$\begin{aligned} m_{jj} + \phi m_{jk} &\geq 0 \\ \phi^2 m_{kk} + \phi m_{jk} &\geq 0 \end{aligned} \tag{47}$$

where m_{kj} has been replaced by m_{jk} since for a symmetric matrix $\mathbf{M}$, m_{kj} is equal to m_{jk}. If ϕ is equal to 1, i.e., two sensor faults of equal magnitude, and taking into account that j and k can be any variable, the two conditions can be reduced to one condition

$$m_{jj} + m_{jk} \geq 0 \qquad \forall j, k \tag{48}$$

which states that each sum of a diagonal element and any other element in the same row or column has to be greater than or equal to zero. Both conditions (Eqs. 47 and 47) are not guaranteed for an arbitrary ϕ and symmetric positive (semi-)definite matrix $\mathbf{M}$, as is proved for the 3×3 case in the next paragraph. The failure of these inequalities will also be illustrated in the numerical example in Section 4.2.

Consider a 3×3 real symmetric matrix $\mathbf{M}$ of the following form

$$\mathbf{M} = \begin{bmatrix} m_{11} & m_{12} & m_{13} \\ m_{12} & m_{22} & m_{23} \\ m_{13} & m_{23} & m_{33} \end{bmatrix} \tag{49}$$

Sylvester's criterion is a necessary and sufficient condition for $\mathbf{M}$ to be positive definite. It states that a matrix is positive definite if and only if the determinants associated with all upper-left submatrices are positive [32]. For the symmetric 3×3 matrix $\mathbf{M}$ this leads to the following three conditions

$$m_{11} > 0 \tag{50}$$

$$m_{11}m_{22} - m_{12}^2 > 0 \tag{51}$$

$$m_{11}m_{22}m_{33} + 2m_{13}m_{12}m_{23} - m_{11}m_{23}^2 - m_{22}m_{13}^2 - m_{33}m_{12}^2 > 0 \tag{52}$$

Journal homepage: http://www.journals.elsevier.com/chemical-engineering-science
Original file available at: http://dx.doi.org/10.1016/j.ces.2013.08.007

Postprint version of paper published in Chemical Engineering Science 2013, vol. 104, p. 285–293.
The content is identical to the published paper, but without the final typesetting by the publisher.

The above conditions do not guarantee the isolatability condition for multiple sensor faults of equal magnitude (Eq. 48) to be true. For example, setting $m_{11} = 1$, $m_{22} = 5$, $m_{22} = 100$ and $m_{12} = m_{13} = m_{23} = -2$ satisfies Sylvester's condition while $m_{11} + m_{12} < 0$. Also the isolatability condition for general multiple sensor faults (Eq. 47) is violated, e.g., for $\{j, k\} = \{1, 2\}$ and $\phi \in]0, \frac{2}{5}[\cup]\frac{1}{2}, +\infty[$. Therefore, correct fault isolation of multiple sensor faults with PD contributions is not guaranteed.

The interpretation of this mathematical result is as follows: although the sum of both contributions equals the value of the fault detection statistic and is positive (or zero), one contribution can be negative, thus smaller than the fault-free contributions. As a consequence, according to the definition of isolatability, correct isolation of multiple sensor faults with PD contributions is not guaranteed as opposed to isolation of single sensor faults.

Isolatability for RB contributions

Similarly, for RB contributions, substituting $\mathbf{x}_{ff}$ in Eq. 17 yields

$$\mathrm{RB}_i = \begin{cases} \dfrac{f^2 \left(m_{ij} + \phi m_{ik}\right)^2}{m_{ii}} & \text{if } i \neq j \wedge i \neq k \\ \dfrac{f^2 \left(m_{jj} + \phi m_{jk}\right)^2}{m_{jj}} & \text{if } i = j \\ \dfrac{f^2 \left(m_{jk} + \phi m_{kk}\right)^2}{m_{kk}} & \text{if } i = k. \end{cases} \tag{53}$$

For correct isolation the contributions of the j-th and k-th variable must be greater than or equal to the contribution of any other variable, resulting in the following necessary and sufficient isolatability condition

$$\begin{aligned} \frac{\left(m_{jj} + \phi m_{jk}\right)^2}{m_{jj}} &\geq \frac{\left(m_{ij} + \phi m_{ik}\right)^2}{m_{ii}} \\ \frac{\left(m_{jk} + \phi m_{kk}\right)^2}{m_{kk}} &\geq \frac{\left(m_{ij} + \phi m_{ik}\right)^2}{m_{ii}} \end{aligned} \tag{54}$$

This condition is not guaranteed for an arbitrary ϕ and symmetric positive (semi-)definite matrix $\mathbf{M}$.

For the 3×3 matrix $\mathbf{M}$ of the previous paragraph, again setting $m_{11} = 1$, $m_{22} = 5$, $m_{22} = 100$ and $m_{12} = m_{13} = m_{23} = -2$ satisfies Sylvester's condition but e.g., for $\{i, j, k\}$ equal to $\{1, 2, 3\}$ and $\phi \in]-\infty, \frac{-(5+3\sqrt{5})}{8}[\cup$

Journal homepage: http://www.journals.elsevier.com/chemical-engineering-science
Original file available at: http://dx.doi.org/10.1016/j.ces.2013.08.007

Postprint version of paper published in Chemical Engineering Science 2013, vol. 104, p. 285–293.
The content is identical to the published paper, but without the final typesetting by the publisher.

$]\frac{-11}{60}, +\infty[$ does not satisfy the RB isolatability condition (Eq. 54). Hence, correct diagnosis with RB contributions is not guaranteed for multiple sensor faults.

As a conclusion, while the PD and RB approaches guaranteed correct isolation of single sensor faults, none of the three contribution methods guarantees correct isolation of multiple sensor faults due to the contribution smearing effect.

4.2. Numerical illustration

The theoretical results of the previous section are derived under the assumption that the normal variation around the average trajectory is negligible compared to the fault magnitude f. This section includes the effect of the fault magnitude on contribution based fault isolation by means of a simulation case study (adapted from [24]).

The Normal Operating Conditions (NOC) data is generated according to the following process model

$$\begin{bmatrix} x_1 \\ x_2 \\ x_3 \\ x_4 \\ x_5 \\ x_6 \end{bmatrix} = \begin{bmatrix} -0.3441 & 0.4815 & 0.6637 \\ -0.2313 & -0.5936 & 0.3545 \\ -0.5060 & 0.2495 & 0.0739 \\ -0.5552 & -0.2405 & -0.1123 \\ -0.3371 & 0.3822 & -0.6115 \\ -0.3877 & -0.3868 & -0.2045 \end{bmatrix} \begin{bmatrix} t_1 \\ t_2 \\ t_3 \end{bmatrix} + \text{noise} \tag{55}$$

where t_1, t_2 and t_3 are uniformly distributed random variables with a range of $[0, 2]$, $[0, 1.6]$ and $[0, 1.2]$, respectively. The noise term consists of white Gaussian noise with zero mean and a standard deviation of 0.2. The simulated single and multiple sensor faults are of the form

$$\mathbf{x}_f = \mathbf{x}_{\text{NOC}} + f\xi_j \tag{56}$$

$$\mathbf{x}_{ff} = \mathbf{x}_{\text{NOC}} + f\xi_j + \phi f\xi_k \tag{57}$$

where $j \neq k$, j and k are uniformly distributed among the six variables and the fault magnitude f has a range of $[0.1, 4]$. Without loss of generality, ϕ is set to 1, i.e., sensor faults of equal magnitude. For each absolute magnitude of f, 3000 faulty samples are generated, 1500 with a negative sign and 1500 having a positive sign. Two thousand NOC samples are generated for model identification. The NOC data is mean-centered and scaled to unit variance. The faulty samples are normalized similarly using the mean and variance of

Journal homepage: http://www.journals.elsevier.com/chemical-engineering-science
Original file available at: http://dx.doi.org/10.1016/j.ces.2013.08.007

Postprint version of paper published in Chemical Engineering Science 2013, vol. 104, p. 285–293.
The content is identical to the published paper, but without the final typesetting by the publisher.

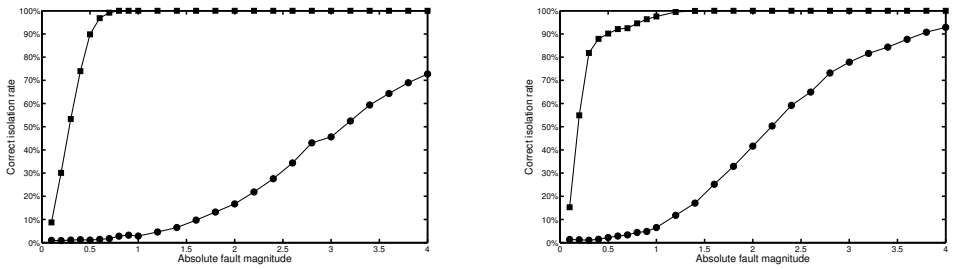

(a) (b)

Figure 1: **Detection rates of the SPE (■) and T^2 (•) statistics for (a) single and (b) multiple faults.**

the NOC data. Three PCA models with respectively 2, 3 and 4 principal components are identified on the NOC data. The faulty samples are subsequently monitored using the SPE and T^2 statistics with a tolerance level α of 1%.

The detection rate of the SPE and T^2 statistics in function of the absolute fault magnitude for single and multiple sensor faults is depicted in Figs. 1(a) and 1(b), respectively, for the PCA model with three principal components. From these figures, it is clear that the SPE statistic has a higher sensitivity for the simulated sensor faults than the T^2 index, reflecting in a higher detection rate for smaller fault magnitudes.

The detection rates depend on the chosen tolerance level α which represents a trade-off between the detection and false alarm rates. To eliminate the influence of the chosen tolerance level on the fault diagnosis results, a detection rate of 100% is assumed. Hence, isolation performance is examined independent from fault detection rates.

Before discussing the numerical fault isolation results, first consider the theoretical isolatability of sensor faults. For example for the 3 component model and SPE statistic

$$\mathbf{M}_{\mathrm{SPE}} = \begin{bmatrix} -0.6729 & -0.1410 & -0.3137 & -0.2982 & -0.1130 & 0.0114 \\ -0.1410 & 0.3537 & 0.0834 & 0.0447 & -0.3554 & 0.2710 \\ -0.3137 & 0.0834 & 0.5685 & -0.3395 & 0.1303 & 0.0876 \\ -0.2982 & 0.0447 & -0.3395 & 0.6744 & -0.0406 & -0.1085 \\ -0.1130 & -0.3554 & 0.1303 & -0.0406 & 0.4853 & -0.3034 \\ 0.0114 & 0.2710 & 0.0876 & -0.1085 & -0.3034 & 0.2452 \end{bmatrix}$$

Journal homepage: http://www.journals.elsevier.com/chemical-engineering-science
Original file available at: http://dx.doi.org/10.1016/j.ces.2013.08.007

Postprint version of paper published in Chemical Engineering Science 2013, vol. 104, p. 285–293.
The content is identical to the published paper, but without the final typesetting by the publisher.

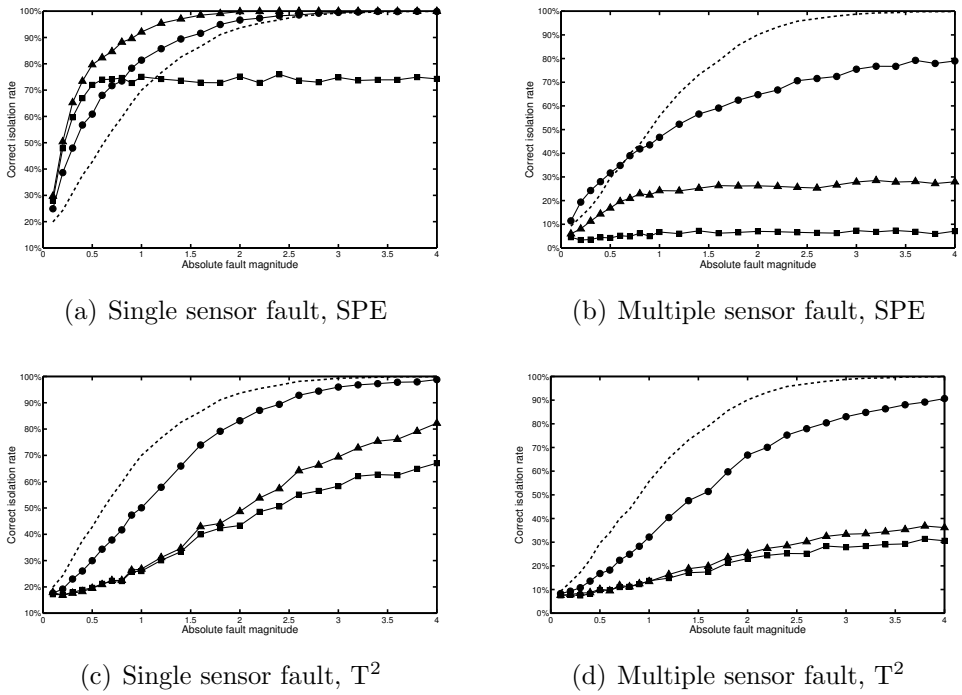

(a) Single sensor fault, SPE

(b) Multiple sensor fault, SPE

(c) Single sensor fault, T^2

(d) Multiple sensor fault, T^2

Figure 2: Correct isolation rates of CD (■), PD (•) and RB contributions (▲) to the SPE index for (a) single and (b) multiple faults and to the T^2 index for (c) single and (d) multiple faults. The dashed line depicts the correct classification rate achieved by using the absolute value of the mean centered and scaled (to unit variance) data.

and it is easy to verify that the isolatability conditions of multiple sensor faults for PD contributions (Eq 48) and RB contributions (Eq. 54) are not satisfied (see e.g., $\{j,k\} = \{5,2\}$ for PD contributions and $\{j,k,i\} = \{1,2,6\}$ for RB contributions). The same conclusions apply to the 2 and 4 component models and the T^2 statistic.

The measured correct fault isolation rates are depicted in Fig. 2. The correct isolation rates of CD (■), PD (•) and RB (▲) contributions to the SPE and T^2 statistics for single sensor faults are plotted in Figs. 2(a) and 2(c), respectively. The contributions are computed from a PCA model with three principal components. The isolation rates are based on all generated samples. The dashed line represents the isolation performance achieved by using the absolute value of the (mean centered and scaled to unit variance) faulty data. The contributions to the T^2 index have lower correct classification

Journal homepage: http://www.journals.elsevier.com/chemical-engineering-science
Original file available at: http://dx.doi.org/10.1016/j.ces.2013.08.007

Postprint version of paper published in Chemical Engineering Science 2013, vol. 104, p. 285–293.
The content is identical to the published paper, but without the final typesetting by the publisher.

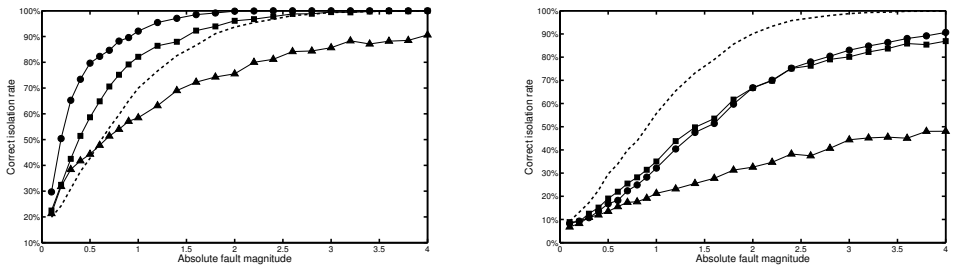

(a) (b)

Figure 3: Correct isolation rates of (a) single sensor faults with RB contributions to the SPE statistic and (b) multiple sensor faults with PD contributions to the T^2 statistic for 2 (■), 3 (●), and 4 (▲) principal components. The dashed line depicts the correct isolation rate achieved by using the absolute value of the mean centered and scaled (to unit variance) data.

rates than those to the SPE index. Be aware that the dashed line does not change between Figs. 2(a) and 2(c) since isolation based on the data is independent of the monitoring statistic used. From the results for the SPE statistic, it is clear that the PD and RB contributions outperform data-based isolation at low fault magnitudes. The RB contributions achieve the highest isolation performance. For larger magnitudes the PD, RB and data-based correct isolation rates reach 100% which is in accordance with the theoretical guarantee of correct isolation for large single sensor faults. On the other hand, correct isolation using CD contributions is not guaranteed and the CD computation method is outperformed by PD and RB.

The correct isolation rates of CD, PD and RB contributions to the SPE and T^2 statistics for multiple sensor faults are plotted in Figs. 2(b) and 2(d), respectively. For multiple sensor faults, data-based isolation (dashed line) has overall higher correct isolation rates. PD contributions achieve the highest performance of the three contribution methods, because they are the most related to the data due to the multiplication of each linear combination with the variables value in Eqs. 38 and 39. CD contributions on the other hand, exhibit the lowest isolation performance. For contributions to the SPE statistic, the CD contributions do not exceed 7% correct isolation rate due to the smearing effect. The RB contributions now take third place, despite having the highest performance for single sensor faults using the SPE index.

The influence of the selected number of principal components r is depicted

Journal homepage: http://www.journals.elsevier.com/chemical-engineering-science
Original file available at: http://dx.doi.org/10.1016/j.ces.2013.08.007

Postprint version of paper published in Chemical Engineering Science 2013, vol. 104, p. 285–293.
The content is identical to the published paper, but without the final typesetting by the publisher.

in Fig. 3 for single sensor faults isolated with RB contributions to the SPE statistic (Fig. 3(a)) and multiple sensor faults isolated with PD contributions to the T^2 statistic (Fig. 3(b)). It is evident from the process model (Eq. 55) that the correct choice of the number of components is 3 since the generated data is governed by 3 latent variables (i.e., t_1, t_2 and t_3). Figs. 3(a) and 3(b) compare the correct isolation rate for the models with 2 (undermodeling), 3 and 4 (overmodeling) components. In Fig. 3(a), r-values different from 3 exhibit a lower correct isolation rate. In Fig. 3(b), the correct isolation rates if r equals 2 or 3 are comparable. For r equal to 4, the performance is significantly lower. Figs. 3(a) and 3(b) is representative for the other combinations of fault type, statistic and contribution computation method. These plots show that under- or overmodelling can have a negative effect on contribution fault isolation performance. Note that the correct isolation rate based on the absolute value of the data (dashed line) is independent of r and is identical to Fig. 2.

As a general conclusion, the PD and RB contributions only outperform direct data based isolation for single sensor faults with small magnitudes. For larger magnitudes and multiple sensor faults, data based isolation has comparable or higher isolation performance, respectively. The use of CD contributions is discouraged since they exhibit the lowest isolation rates, even failing to achieve 100% correct isolation for large single sensor faults. A poorly chosen number of principal components may lower isolation performance of contribution plots while data-based isolation remains unaffected.

5. Smearing revisited

In literature, the general stance on contribution smearing is that it has a negative effect on fault isolation by potentially highlighting normal variables and obscuring faulty variables [1, 31, 33]. Therefore, different authors have either (*i*) warned that contribution plots should be interpreted with care due to smearing or (*ii*) proposed new approaches to contribution computation which are claimed to be less affected by smearing e.g., alternative decompositions of fault detection statistics [34, 35], reconstruction-based contributions [25] and iterative approaches to identify a subset of contributing variables [36].

Fault isolation confines the origin of a detected fault to a subset of the measured variables and in this way greatly narrows the search for the underlying cause. However, fault isolation is only a starting point: operators and

Journal homepage: http://www.journals.elsevier.com/chemical-engineering-science
Original file available at: http://dx.doi.org/10.1016/j.ces.2013.08.007

Postprint version of paper published in Chemical Engineering Science 2013, vol. 104, p. 285–293.
The content is identical to the published paper, but without the final typesetting by the publisher.

plant engineers still need to bridge the gap between the fault isolation results and true fault diagnosis. Fault isolation techniques should aim to minimize this gap. Because PCA or PLS based techniques only model correlation, not causation, contribution plots highlight groups of correlated variables, which is the essence of contribution smearing.

The previous analysis (Section 3) shows that to eliminate the smearing effect, the coefficients $\gamma_{i,j}$, $\delta_{i,j}$ and $\zeta_{i,j}$ in Eqs. 25, 26, 38, 39, 42 and 43 simply have to be set to zero, i.e., multivariate detection followed by univariate fault isolation. Hence, univariate fault isolation is superior to contribution plots when smearing presents a problem for fault isolation.

If a physical interpretation of the principal components is available, it is advisable to base the fault isolation on the deviation of the current scores $\mathbf{t}$ from those obtained under normal operating conditions. Isolating a detected disturbance to one or more scores allows one to link the detected disturbance with the underlying process dynamics captured by the principal components corresponding to these scores. In this case, the result of the fault isolation step is a group of variables corresponding to the faulty dynamics, rather than individual variables. Knowing what process dynamics are faulty provides operators with a good starting point to bridge the gap to true fault diagnosis based on their process experience.

Unfortunately, a clear physical interpretation of each score is seldom available for process data. Section 3 demonstrated that the linear combination present at the core of each contribution computation method evidences the presence of smearing. The coefficients of this linear combination depend heavily on the principal components. If the interpretation of the principal components is unclear, using this information for fault isolation may confuse operators and increase the gap between isolation and diagnosis. The case study results (Section 4) have shown that the information contained in the principal components might be helpful for example when isolating single sensor faults with the RB technique, but might obscure the faulty variables for faults as relatively simple as multiple sensor faults where data based isolation achieves much higher correct isolation rates. Therefore, if no clear interpretation of the principal components is available, the authors advise to discard this information and perform univariate fault isolation, i.e., basing fault isolation of general process faults on the deviation of the current measurements from their NOC values instead of contributions or scores.

Journal homepage: http://www.journals.elsevier.com/chemical-engineering-science
Original file available at: http://dx.doi.org/10.1016/j.ces.2013.08.007

Postprint version of paper published in Chemical Engineering Science 2013, vol. 104, p. 285–293.
The content is identical to the published paper, but without the final typesetting by the publisher.

6. Conclusion

Contribution plots are widely used in applications for fault isolation in conjunction with PCA or PLS based fault detection. Despite their popularity, contribution plots suffer from the so-called smearing effect, i.e., the propagation of faulty variables' contributions to those of variables not influenced by the fault. As a consequence, non-faulty variables may be highlighted and faulty obscured in the contribution plots, which complicates the fault isolation task.

This paper presented an analysis of the smearing effect for three general contribution computation methods: complete decomposition (CD), partial decomposition (PD) and reconstruction-based (RB) contributions. From the analysis three main conclusions can be drawn: (*i*) the linear combination at the core of each contribution computation method evidences the presence of smearing, (*ii*) the contributions depend on the selected model order of the underlying PCA or PLS model and (*iii*) the extent of smearing between variables tends to increase as the variables are more correlated in the NOC data provided the model order is high enough to adequately reflect the NOC covariance matrix.

The effect of smearing on fault isolation performance was further studied for the specific case study of sensor faults. While previous work has shown that correct isolation is guaranteed for PD and RB contributions in the case of large magnitude single sensor faults, this paper demonstrated that correct isolation is not guaranteed for multiple sensor faults. The isolation performance of the three contribution methods was tested via a simulation case study and referenced against the isolation performance achieved by isolating the variables with the largest absolute auto-scaled values, i.e., multivariate detection followed by univariate fault isolation. For single sensor faults with small magnitudes, the PD and RB methods outperform data-based isolation. However, for larger fault magnitudes the isolation performance is similar and for multiple sensor faults the contribution methods are clearly outperformed by looking directly at the data due to the smearing effect.

Since, according to the smearing analysis results, smearing mainly occurs through the principal components, the authors discourage the use of contribution plots if a physical interpretation of the principal components is unavailable, which is often the case for process data, and advise to base the isolation task on the deviation of each variable from its expected value, i.e., univariate fault isolation. Whenever a clear physical interpretation of the

Journal homepage: http://www.journals.elsevier.com/chemical-engineering-science
Original file available at: http://dx.doi.org/10.1016/j.ces.2013.08.007

principal components is available, it is advisable to base the fault isolation task on the current scores since these allow to link the detected disturbance with one or more of the underlying process dynamics captured by the principal components.

Acknowledgements

Work supported in part by Project PVF/10/002 (OPTEC Optimization in Engineering Center) of the Research Council of the KU Leuven, Project KP/09/005 (SCORES4CHEM) of the Industrial Research Council of the KU Leuven, and the Belgian Program on Interuniversity Poles of Attraction initiated by the Belgian Federal Science Policy Office. P. Van den Kerkhof and J. Vanlaer are funded by a Ph.D grant of the agency for Innovation by Science and Technology (IWT). J. Van Impe holds the chair Safety Engineering sponsored by the Belgian chemistry and life sciences federation essenscia. The authors assume scientific responsibility.

1. Westerhuis, J., Gurden, S., Smilde, A.. Generalized contribution plots in multivariate statistical process monitoring. *Chemometrics and Intelligent Laboratory Systems* 2000;**51**:95–114.

2. Al Ghazzawi, A., Lennox, B.. Monitoring a complex refining process using multivariate statistics. *Control Engineering Practice* 2008;**16**:294–307.

3. Bezergianni, S., Kalogianni, A.. Application of principal component analysis for monitoring and disturbance detection of a hydrotreating process. *Industrial & Engineering Chemistry Research* 2008;**47**:6972–6982.

4. Tates, A., Louwerse, D., Smilde, A., Koot, G., Berndt, H.. Monitoring a PVC batch process with multivariate statistical process control charts. *Industrial & Engineering Chemistry Research* 1999;**38**:4769–4776.

5. Schlags, C., Populе, M.. Industrial application of SPC to batch polymerization processes. *Proceedings of the American Control Conference* 2001;.

6. Berber, R., Atasoy, I., Yuceer, M., Deniz, G.. On-line statistical process monitoring and fault diagnosis in batch bakers yeast fermentation. *Chem Eng Technol* 2009;**32**(4):650–658.

Journal homepage: http://www.journals.elsevier.com/chemical-engineering-science
Original file available at: http://dx.doi.org/10.1016/j.ces.2013.08.007

7. Bissessur, Y., Martin, E., Morris, A.. Monitoring the performance of the paper making process. *Control Engineering Practice* 1999;**7**:1357–1368.

8. Zhang, Y., Dudzic, M.. Online monitoring of steel casting processes using multivariate statistical technologies: From continuous to transitional operations. *Journal of Process Control* 2006;**16**:819–829.

9. Zhang, Y., Dudzic, M.. Industrial application of multivariate spc to continuous caster start-up operations for breakout prevention. *Control Engineering Practice* 2006;**14**:1357–1375.

10. Jollife, I.. *Principal Component Analysis*. Springer Verlag; 1986.

11. Geladi, P., Kowalski, B.. Partial Least-Squares Regression: a tutorial. *Analytica Chimica Acta* 1986;**185**:1–17.

12. Kresta, J., MacGregor, J., Marlin, T.. Multivariate statistical monitoring of processes. *Canadian Journal of Chemical Engineering* 1991; **69**(1):35–47.

13. Nomikos, P., MacGregor, J.. Multi-way partial least squares in monitoring batch processes. *Chemometrics and Intelligent Laboratory Systems* 1995;**30**:97–108.

14. Ku, W., Storer, R., Georgakis, C.. Disturbance detection and isolation by dynamic principal component analysis. *Chemometrics and Intelligent Laboratory Systems* 1995;**30**:179–196.

15. Chen, J., Liu, K.. On-line batch process monitoring using dynamic PCA and dynamic PLS models. *Chemical Engineering Science* 2002; **57**(1):63–75.

16. Choi, S., Morris, J., I.-B. Lee, . Dynamic model-based batch process monitoring. *Chemical Engineering Science* 2008;**63**:622–636.

17. J.-M. Lee, , Yoo, C., I.-B. Lee, . Fault detection of batch processes using multiway kernel principal component analysis. *Computers & Chemical Engineering* 2004;**28**:1837–1847.

Journal homepage: http://www.journals.elsevier.com/chemical-engineering-science
Original file available at: http://dx.doi.org/10.1016/j.ces.2013.08.007

18. Kim, K., J.-M. Lee, , I.-B. Lee, . A novel multivariate regression approach based on kernel partial least squares with orthogonal signal correction. *Chemometrics and Intelligent Laboratory Systems* 2005;**79**:22–30.

19. Miller, P., Swanson, R., Heckler, C.. Contribution plots: a missing link in multivariate quality control. *Applied Mathematics and Computer Science* 1998;**8**:775–792.

20. Weighell, M., Martin, E., Morris, A.. The statistical monitoring of a complex manufacturing process. *Journal of Applied Statistics* 2001; **28**(3-4):409–425.

21. Jackson, J.. *A user's guide to Principal Component Analysis*. John Wiley & Sons; 1991.

22. MacGregor, J., Jaeckle, C., Kiparissides, C., Koutoudi, M.. Process monitoring and diagnosis by multiblock PLS methods. *AIChE Journal* 1994;**40**(5):826–838.

23. MacGregor, J., Kourti, T.. Statistical process control of multivariate processes. *Control Engineering Practice* 1995;**3**(3):403–414.

24. Alcala, C., Qin, S.. Analysis and generalization of fault diagnosis methods for process monitoring. *Journal of Process Control* 2011;**21**:322–330.

25. Alcala, C., Qin, S.. Reconstruction-based contribution for process monitoring. *Automatica* 2009;**45**:1593–1600.

26. Dunia, R., Qin, S.. Subspace approach to multidimensional fault identification and reconstruction. *AIChE Journal* 1998;**44**:1813–1831.

27. Yue, H., Qin, S.. Reconstruction-based fault identification using a combined index. *Industrial & Engineering Chemistry Research* 2001; **40**(20):4403–4414.

28. Arteaga, F., Ferrer, A.. Dealing with missing data in MSPC: several methods, different interpretations, some examples. *Journal of Chemometrics* 2002;**16**:408–418.

Journal homepage: http://www.journals.elsevier.com/chemical-engineering-science
Original file available at: http://dx.doi.org/10.1016/j.ces.2013.08.007

29. Lieftucht, D., Kruger, U., Irwin, G.. Improved reliability in diagnosing faults using multivariate statistics. *Computers & Chemical Engineering* 2006;**30**:901–912.

30. Lieftucht, D., Völker, M., Sonntag, C., Kruger, U., Irwin, G., Engell, S.. Improved fault diagnosis in multivariate systems using regression-based reconstruction. *Control Engineering Practice* 2009;**17**:478–493.

31. Yoon, S., MacGregor, J.. Fault diagnosis with multivariate statistical models part I: using steady state fault signatures. *Journal of Process Control* 2001;**11**:387–400.

32. Horn, R., Johnson, C.. *Matrix analysis*. Cambridge University Press; 1985, p. 404.

33. Qin, S.. Statistical process monitoring: basics and beyond. *Journal of Chemometrics* 2003;**17**:480–502.

34. Alvarez, C., Brandolin, A., Sánchez, M.. On the variable contributions to the D-statistic. *Chemometrics and Intelligent Laboratory Systems* 2007;**88**:189–196.

35. Mnassri, B., El Adel, E., Ouladsine, M.. Fault localization using principal component analysis based on a new contribution to the squared prediction error. In: *16th Mediterranean Conference on Control and Automation*. 2008, p. 65–70.

36. Kariwala, V., P.-E. Odiowei, , Cao, Y., Chen, T.. A branch and bound method for isolation of faulty variables through missing variable analysis. *Journal of Process Control* 2010;**20**:1198–1206.

Journal homepage: http://www.journals.elsevier.com/chemical-engineering-science
Original file available at: http://dx.doi.org/10.1016/j.ces.2013.08.007